Thin-Walled Structures 179 (2022) 109755

Contents lists available at ScienceDirect

Thin-Walled Structures

journal homepage: www.elsevier.com/locate/tws

Full length article

Large deflection of multilayer sandwich beams with foam-filled trapezoidal corrugated and foam cores

Jianxun Zhang [a,b,*], Hao Sun [a], Jinlong Du [a], Xiaoming Liu [b], Zhimin Xu [c], Wei Huang [a]

[a] State Key Laboratory for Strength and Vibration of Mechanical Structures, School of Aerospace Engineering, Xi'an Jiaotong University, Xi'an 710049, China
[b] State Key Laboratory of Nonlinear Mechanics, Institute of Mechanics, Chinese Academy of Sciences, Beijing 100190, China
[c] National Mechanics Experimental Teaching Demonstration Center, School of Aerospace Engineering, Xi'an Jiaotong University, Xi'an 710049, China

ARTICLE INFO

Keywords:
Multilayer sandwich beam
Foam-filled trapezoidal corrugated core
Yield criterion
Large deflection
Energy absorption

ABSTRACT

The paper used the analytical and numerical methods to analyze large deflection of multilayer sandwich beams with foam-filled trapezoidal corrugated and foam cores. Considering both the strength of metal foam and corrugated core, we obtained a yield criterion for the multilayer sandwich structure foam-filled trapezoidal corrugated and foam cores. Based on proposed yield criterion, we further presented an analytical solution for large deflection of such multilayer sandwich beam under transverse loading. Well agreement is achieved between analytical and numerical results. What is more, we discussed the effects of foam strength, punch size, face-sheet thickness and middle foam thickness on the plastic behaviors.

1. Introduction

Sandwich structures are widely used in transportation, aerospace and other fields because of the high specific stiffness and strength and lightweight compared with traditional structures. Several core materials have been developed, such as metal foam, honeycomb, corrugated core and pyramid truss [1–10]. The core material design of the sandwich structure is an important aspect of the sandwich structure, which mainly affects the mechanical properties of the sandwich structure under different loads. The reasonable core material design can significantly reduce the weight of sandwich structure. Metal foam sandwich structures are widely used as energy-absorbing components due to the long platform stress, while the bearing capacity is low before the densification due to relatively low peak loads [11]. Also, corrugated sandwich structures have been widely used due to the high peak loads, while the energy absorption performance has certain limitations, as the load usually decreases rapidly after reaching the peak [12]. The energy absorption capacity of the design multilayer sandwich structures is significantly greater than that of the single-layer sandwich structure [13]. In order to combine the advantages of the foam and corrugated sandwich structures, the multilayer sandwich structure with foam-filled trapezoidal corrugated and foam cores is designed. It is necessary to study the load-carrying capacity of the clamped multilayer sandwich structure with foam-filled trapezoidal corrugated and foam cores.

In the past decades, the quasi-static mechanical behavior of sandwich structures has been widely studied. Gibson et al. [14] studied and summarized the stiffness, strength and failure mechanism diagram of sandwich beams under quasi-static loading, which laid a foundation for the follow-up research of sandwich beams. Tagarielli et al. [15] experimentally studied the failure modes of clamped and simply supported composite sandwich beams with glass vinyl resin face-sheets and PVC foam core under three-point bending, and gave the initial critical load formula of failure modes. Yu et al. [16] conducted quasi-static bending tests on aluminum foam sandwich beams, observed failure modes, and conducted the failure mechanism maps. Cruip et al. [17] experimentally studied the static bending behavior of two aluminum honeycomb sandwich structures with different honeycomb sizes, and the experimental results show that the energy absorption of sandwich beam is greatly affected by honeycomb size. Jing et al. [18] studied the structural response of open cell aluminum foam sandwich beams under quasi-static loading. Zhang et al. [19] carried out quasi-static compression test on carbon fiber reinforced polymer sandwich structures with pyramidal truss cores, and the test results show that the low-density aluminum alloy pyramidal truss core has superior energy absorption capacity. Jiang et al. [20] established analytical solutions of the critical loads for failure modes of foam core sandwich beams under three-point bending. More investigations focus on the bending behaviors of sandwich structures under three-point bending, such as Tagarielli et al. [15], Yu et al. [16], Cruip et al. [17], Jiang et al. [20]. Tagarielli et al. [15] focus on the bending behaviors of clamped sandwich beams, and the boundary condition and loading are same as those of the present work.

* Corresponding author at: State Key Laboratory for Strength and Vibration of Mechanical Structures, School of Aerospace Engineering, Xi'an Jiaotong University, Xi'an 710049, China.
E-mail address: jianxunzhang@mail.xjtu.edu.cn (J.X. Zhang).

https://doi.org/10.1016/j.tws.2022.109755
Received 10 November 2021; Received in revised form 29 May 2022; Accepted 5 July 2022
Available online 17 July 2022
0263-8231/

Mechanical properties of foam-filled core sandwich structures have been studied. Nia et al. [21] studied the effect of filled foam on plastic behavior and mechanical properties of the honeycomb panels, the tests show that the average compressive strength of foam-filled panels is greater than the sum of average compressive strengths of honeycomb and foam. Mahmoudabadi et al. [22] established a theoretical model of the average compressive strength of foam-filled metal honeycomb under quasi-static loading, and experimental results show that the average crushing stress of foam-filled honeycomb is nearly 30% higher than that sum of honeycomb and foam. Burlayenko et al. [23] investigated the foam-filling influence on the elastic behavior of the honeycomb structure through theoretical analysis and finite element simulation, and found that the foam increases the stiffness of the sandwich panels, enhances the resistance to the damage caused by debonding. Zhang et al. [24] investigated the deformation and failure mechanisms of pyramidal lattice core sandwich panels filled with polyurethane foam under quasi-static compressive load, and found that the load-carrying capacity of foam-filled pyramidal lattice core sandwich plates can exceed the sum of the unfilled specimens and the filled polyurethane block. Zhang et al. [25] obtained the analytical solution of the clamped foam-filled sinusoidal corrugated sandwich beams under impulsive loading based on the plastic string. Qin et al. [26] analytically and numerically studied the quasi-static and dynamic response of fully clamped corrugated sandwich beam with metal foam-filled folded plate core under low-velocity impact. Fu et al. [27] experimentally studied flexural and shear characteristics of bio-based sandwich panels made of fiber-reinforced polymer skins and foam-filled paper honeycomb core under four-point bending, the results show that the specimens with foam-filled paper honeycomb cores showed a higher load capacity than those with hollow honeycomb cores.

Designed multilayer sandwich structure may be more effective than single-layer sandwich structure in energy absorption, and multilayer sandwich structure has different properties, which provides more choices for structural design. Sha et al. [28] studied the deformation and damage mechanism of sandwich beams and multilayer beams with aluminum foam core and metal face-sheets under four-point bending, and observed local denting and core shear failure modes. Apetre et al. [29] studied low-velocity impact of sandwich beams with functionally graded core, and numerical results show reasonable graded core design can effectively reduce shear force and strain in structure. Xiong et al. [30] studied the failure mechanism and energy absorption of double-layer carbon fiber composite sandwich plates with pyramidal-core through quasi-static uniform compression test and low-velocity impact test. Kilicaslan et al. [31] studied the quasi-static and dynamic axial compressive tests of multilayer corrugated core sandwich structures by experimental and numerical methods, it was found the multilayer core material reduces the buckling stress and increases the compact strain. Hou et al. [32] conducted quasi-static compressive test and numerical simulation on the multilayer metal corrugated sandwich plate with trapezoidal aluminum core, results show that the number of layers have an important effect on the failure mechanism and energy absorption. Cao et al. [33] experimentally investigated multilayer corrugated core sandwiches under out-of-plane compressive impact loading, and found the bending of interlayer for parallel multilayer sandwiches leads to a better extra layer interaction and reduces the force oscillation during the successive folding. Zhang et al. [34] analytically and numerically investigated the large deflection of fully clamped multilayer sandwich beams with metal foam cores, and the analytical and numerical results are verified by each other. Zhou et al. [35] analytically and numerically investigated the large deflection of a slender functionally graded beam under transverse loading. Ferdous et al. [36] experimentally and numerically studied flexural behavior of layered sandwich beams consists of glass fiber reinforced polymer skins and phenolic cores, and results show that the bending strength of vertical layered sandwich beam were improved compared with that of single sandwich beam. Li et al. [37] experimentally and numerically studied dynamic crushing and energy absorption of foam-filled multilayer folded structures, observed the core collapse, and significantly improved the average compressive capacity. Shu et al. [38] analyzed the crashworthiness of multilayer corrugated sandwich panels with different core types, arrangement modes, geometrical parameters, and determined the optimal configuration by orthogonal experimental design and range analysis. Zhou et al. [39] studied the dynamic response of clamped graded metal foam core sandwich plates under blast loading, and found that the homogeneous core material is better than the gradient core material with the equal mass. MacDonnell et al. [40] studied the flexural and shear properties of sandwich beams fabricated with layered cores and glass fiber-reinforced polymer composite facings through experiments and theoretical analysis, and developed an analytical model to predict the failure loading. To sum up, the investigations on the yield criterion and large deflection of multilayer sandwich beam with foam-filled trapezoidal corrugated and foam cores were not reported publicly.

The objective of this work is to investigate the yield criterion and large deflection of multilayer sandwich beams with foam-filled trapezoidal corrugated and foam cores. In Section 2, the problem formulation is presented. In Section 3, the yield criterion of the multilayer sandwich structure with foam-filled trapezoidal corrugated and foam cores is derived, considering strengths of metal foam and corrugated core. In Section 4, analytical solutions are derived for the multilayer sandwich beam with foam-filled trapezoidal corrugated and foam cores transversely loaded by a flat punch. In Section 5, comparisons between analytical and numerical results are performed. The effects of foam strength, punch size, face-sheet thickness on the plastic behavior of the multilayer sandwich beams with foam-filled trapezoidal corrugated and foam cores are discussed in details. Finally, concluding remarks are presented.

2. Problem formulation

Consider a fully clamped multilayer sandwich beam with foam-filled trapezoidal corrugated and foam cores under transverse loading by a flat punch of length $2a$, as depicted in Fig. 1. The span of the multilayer sandwich beam is $2L$, the thickness of the identical face-sheet and interlayer plate is h, the height of top and bottom foam-filled trapezoidal corrugated cores is c, the height of metal foam core is c_m. All parts are assumed to be perfect bonding. Sketches of multilayer sandwich beam with foam-filled trapezoidal corrugated and foam cores, the half unit cell of multilayer sandwich beam are shown in Fig. 2(a) and (b).

The width of the half unit cell is denoted as b, the thickness and the angle of inclination of the trapezoidal corrugated core plate are b_c and θ. The densities of face-sheets, corrugated core and metal foam core are ρ_f, ρ_{fc} and ρ_c, respectively. It is assumed that face-sheets and corrugated cores obey rigid-perfectly plastic material with yield strengths σ_f and σ_{fc}, and metal foam core follows rigid-perfectly plastic-locking material with yield strength σ_c and densification strain ε_D.

3. Yield criterion

Consider a multilayer sandwich cross-section with foam-filled trapezoidal corrugated and foam cores. It is assumed that the sandwich cross-section has a fully plastic stress distribution resulting from a combination of bending moment M and axial force N. Fig. 3 shows the distributions of the strain and stress on cross-section of the multilayer sandwich beam with foam-filled trapezoidal corrugated and foam cores. The distance between the plastic neutral surface and the outer surface of the bottom face-sheet is denoted by $H = \xi\left(4h + 2c + c_m\right)$, where $\xi \in [0, 1]$. According to the difference position of the plastic neutral surface, the relationship between the axial force and bending moment can be divided into six cases. In Fig. 3(a), when $0 \le \xi \le \frac{h}{4h+2c+c_m}$, the

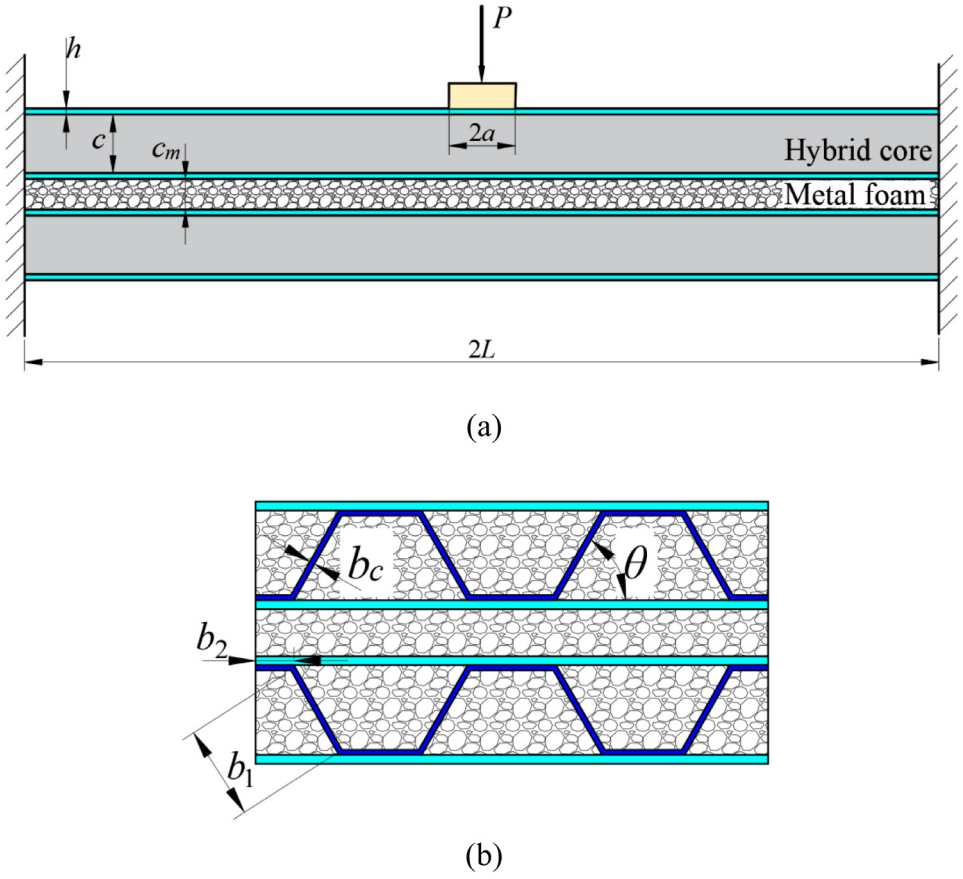

Fig. 1. (a) Sketch of a fully clamped multilayer sandwich beam with foam-filled trapezoidal corrugated and foam cores under transverse loading by a flat punch, and (b) the cross-section for multilayer sandwich beam with foam-filled trapezoidal corrugated and foam cores.

axial force N and the bending moment M of the multilayer sandwich cross-section with foam-filled trapezoidal corrugated and foam cores can be given by

$$\begin{aligned} N &= \int_A \sigma dA \\ &= 2\sigma_f b\left[2h - \xi(4h + 2c + c_m)\right] + \sigma_c b(2c + c_m) + 2(\sigma_{fc} - \sigma_c)(b_1 + 2b_2)b_c \end{aligned} \tag{1}$$

and

$$M = \int_A \sigma z dA = \sigma_f b\left(4h + 2c + c_m\right)^2\left(\xi - \xi^2\right) \tag{2}$$

respectively. See Appendix for details of other cases.

The fully plastic axial force N_P and bending moment M_P correspond to $\xi = 0$ and $\xi = 1/2$,

$$N_P = 4\sigma_f bh + \sigma_c b(2c + c_m) + 2(\sigma_{fc} - \sigma_c)(b_1 + 2b_2)b_c \tag{3}$$

and

$$\begin{aligned} M_P &= \sigma_f bh\left(4h + 2c + 2c_m\right) \\ &\quad + \left[\sigma_c bc + \left(\sigma_{fc} - \sigma_c\right) b_c\left(b_1 + 2b_2\right)\right]\left(2h + c + c_m\right) + \frac{1}{4}\sigma_c bc_m^2 \end{aligned} \tag{4}$$

Eliminating the parameter ξ of Eqs. (A.11) and (A.12), the yield criterion of the multilayer sandwich cross-section with foam-filled trapezoidal corrugated and foam cores can be written as

$$|m| = \begin{cases} 1 - \dfrac{(An)^2}{4\overline{\sigma}_c B}, & 0 \le |n| \le \dfrac{\overline{\sigma}_c \overline{c}_m}{A} \\ \dfrac{4C_1 - \left(\overline{c}_m - \overline{\sigma}_c \overline{c}_m + A|n|\right)^2}{4B}, & \dfrac{\overline{\sigma}_c \overline{c}_m}{A} \le |n| \le \dfrac{2\overline{h} + \overline{\sigma}_c \overline{c}_m}{A} \\ \dfrac{8C_3C_4 - \left(4\overline{h} + 1\right)\left(C_3 - 2C_2 + 2A|n|\right)^2}{8BC_3}, & \dfrac{2\overline{h} + \overline{\sigma}_c \overline{c}_m}{A} \le |n| \le \dfrac{D_1}{A} \\ \dfrac{8C_6C_7 - \left(4\overline{h} + 1\right)\left(C_6 - 2C_5 + 2A|n|\right)^2}{8BC_6}, & \dfrac{D_1}{A} \le |n| \le \dfrac{D_2}{A} \\ \dfrac{8C_9C_{10} - \left(4\overline{h} + 1\right)\left(C_9 - 2C_8 + 2A|n|\right)^2}{8BC_9}, & \dfrac{D_2}{A} \le |n| \le \dfrac{A - 2\overline{h}}{A} \\ \dfrac{2A(1 - |n|)(4\overline{h} + 1) - A^2(1 - |n|)^2}{4B}, & \dfrac{A - 2\overline{h}}{A} \le |n| \le 1 \end{cases} \tag{5}$$

where

$$A = 4\overline{h} + \overline{\sigma}_c + 2\left(\overline{\sigma}_{fc} - \overline{\sigma}_c\right)\overline{b}_c\left(\overline{b}_1 + 2\overline{b}_2\right),$$

$$\begin{aligned} B &= \overline{h}\left(4\overline{h} + 1 + \overline{c}_m\right) + \left[\overline{\sigma}_c \overline{c} + \left(\overline{\sigma}_{fc} - \overline{\sigma}_c\right)\overline{b}_c\left(\overline{b}_1 + 2\overline{b}_2\right)\right]\left(2\overline{h} + \overline{c} + \overline{c}_m\right) \\ &\quad + \frac{1}{4}\overline{\sigma}_c \overline{c}_m^2, \end{aligned}$$

$$\begin{aligned} C_1 &= \overline{h}\left(3\overline{h} + 1\right) + \frac{1}{4}\left(2\overline{h} + \overline{c}_m\right)^2 \\ &\quad + \left[\overline{\sigma}_c \overline{c} + \left(\overline{\sigma}_{fc} - \overline{\sigma}_c\right)\overline{b}_c\left(\overline{b}_1 + 2\overline{b}_2\right)\right]\left(2\overline{h} + \overline{c} + \overline{c}_m\right), \end{aligned}$$

$$C_2 = 2\overline{h} + \overline{\sigma}_c\left(1 + 2\overline{h}\right) + 2\left(\overline{\sigma}_{fc} - \overline{\sigma}_c\right)\overline{b}_{21}\left(\overline{h} + \overline{c}\right),$$

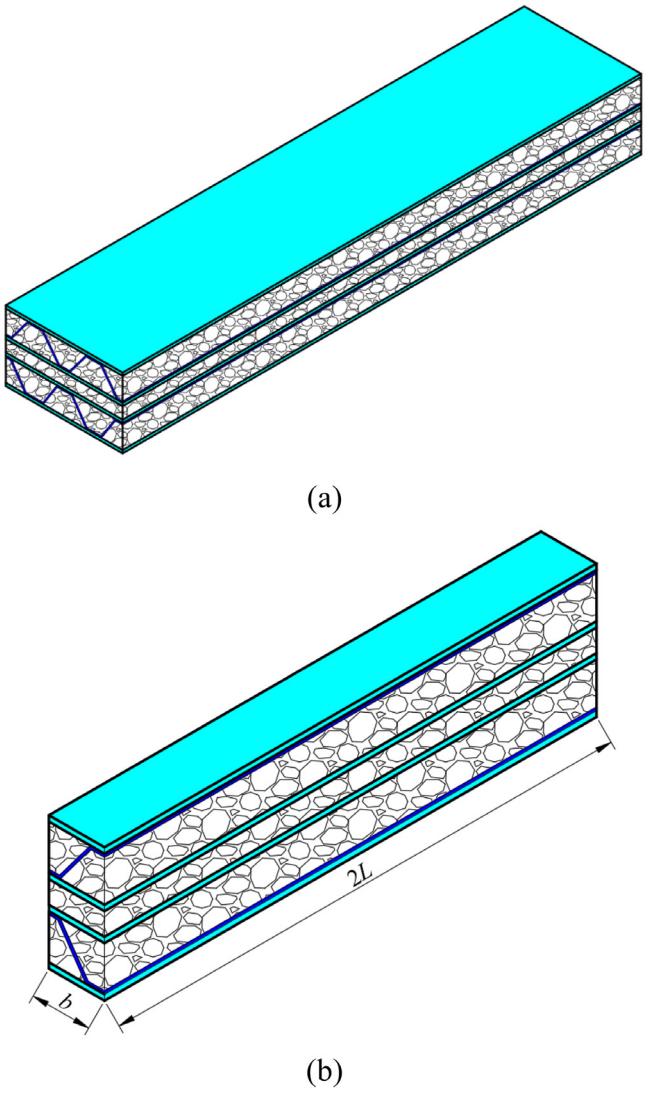

Fig. 2. (a) Sketches of the multilayer sandwich beam with foam-filled trapezoidal corrugated and foam cores and (b) half unit cell for the multilayer sandwich beam with foam-filled trapezoidal corrugated and foam cores.

$$C_3 = 2\bar{\sigma}_c\left(4\bar{h}+1\right)+2\left(\bar{\sigma}_{fc}-\bar{\sigma}_c\right)\bar{b}_{21}\left(4\bar{h}+1\right),$$

$$C_4 = \bar{h}\left(3\bar{h}+1\right)+\frac{1}{4}\bar{\sigma}_c\left(2\bar{h}+1\right)^2+\left(\bar{\sigma}_{fc}-\bar{\sigma}_c\right)\left[\bar{b}_c\bar{b}_2\left(2\bar{h}+1-\bar{b}_{c1}\right)+\bar{b}_c\bar{b}_1\left(2\bar{h}+\bar{c}+\bar{c}_m\right)+\frac{1}{4}\bar{b}_{21}\left(2\bar{h}+2\bar{b}_{c1}+\bar{c}_m\right)^2\right],$$

$$C_5 = 2\bar{h}+\bar{\sigma}_c\left(1+2\bar{h}\right)+2\left(\bar{\sigma}_{fc}-\bar{\sigma}_c\right)\bar{b}_c\left[\bar{b}_1+\bar{b}_2+\left(\bar{h}+\bar{b}_{c1}\right)/\sin\theta\right],$$

$$C_6 = 2\bar{\sigma}_c\left(4\bar{h}+1\right)+2\left(\bar{\sigma}_{fc}-\bar{\sigma}_c\right)\left(4\bar{h}+1\right)\bar{b}_c/\sin\theta,$$

$$C_7 = \bar{h}\left(3\bar{h}+1\right)+\frac{1}{4}\bar{\sigma}_c\left(2\bar{h}+1\right)^2+\left(\bar{\sigma}_{fc}-\bar{\sigma}_c\right)\bar{b}_c\bar{b}_2\left(2\bar{h}+1-\bar{b}_{c1}\right)+\frac{1}{4}\left(\bar{\sigma}_{fc}-\bar{\sigma}_c\right)\frac{\bar{b}_c}{\sin\theta}\left(2\bar{h}+1-2\bar{b}_{c1}\right)^2,$$

$$C_8 = 2\bar{h}+\bar{\sigma}_c\left(1+2\bar{h}\right)+2\left(\bar{\sigma}_{fc}-\bar{\sigma}_c\right)\left[\bar{b}_c\left(\bar{b}_1+2\bar{b}_2\right)+\bar{b}_{21}\bar{h}\right],$$

$$C_9 = C_3 = 2\bar{\sigma}_c\left(4\bar{h}+1\right)+2\left(\bar{\sigma}_{fc}-\bar{\sigma}_c\right)\bar{b}_{21}\left(4\bar{h}+1\right),$$

$$C_{10} = \bar{h}\left(3\bar{h}+1\right)+\frac{1}{4}\left[\bar{\sigma}_c+\left(\bar{\sigma}_{fc}-\bar{\sigma}_c\right)\bar{b}_{21}\right]\left(2\bar{h}+1\right)^2,$$

$$D_1 = 2\bar{h}+\bar{\sigma}_c\left(\bar{c}_m+2\bar{b}_{c1}\right)+2\bar{b}_c\bar{b}_2\left(\bar{\sigma}_{fc}-\bar{\sigma}_c\right),$$

$$D_2 = 2\bar{h}+\bar{\sigma}_c\left(1-2\bar{b}_{c1}\right)+2\left(\bar{\sigma}_{fc}-\bar{\sigma}_c\right)\bar{b}_c\left(\bar{b}_1+\bar{b}_2\right).$$

Particularly, when $\sigma_f = \sigma_{fc} = \sigma_c$, which corresponds to a monolithic solid structure, Eq. (5) is reduced to the yield criterion of the monolithic rectangular solid cross-section [41],

$$|m| + n^2 = 1 \tag{6}$$

Fig. 4 shows the yield loci of multilayer sandwich cross-sections with foam-filled trapezoidal corrugated and foam cores with various foam strengths.

On this basis, the unified yield criterion and associated plastic flow rule would be employed to derive the analytical solutions for large deflections of the fully clamped multilayer sandwich beam with foam-filled trapezoidal corrugated and foam cores, in which the interaction of bending and stretching is considered.

4. Analytical solutions for large deflection of the multilayer sandwich beam

Here, the large deflection of a fully clamped multilayer sandwich beam with foam-filled trapezoidal corrugated and foam cores under transverse loading by a flat punch is derived. It is assumed that slender

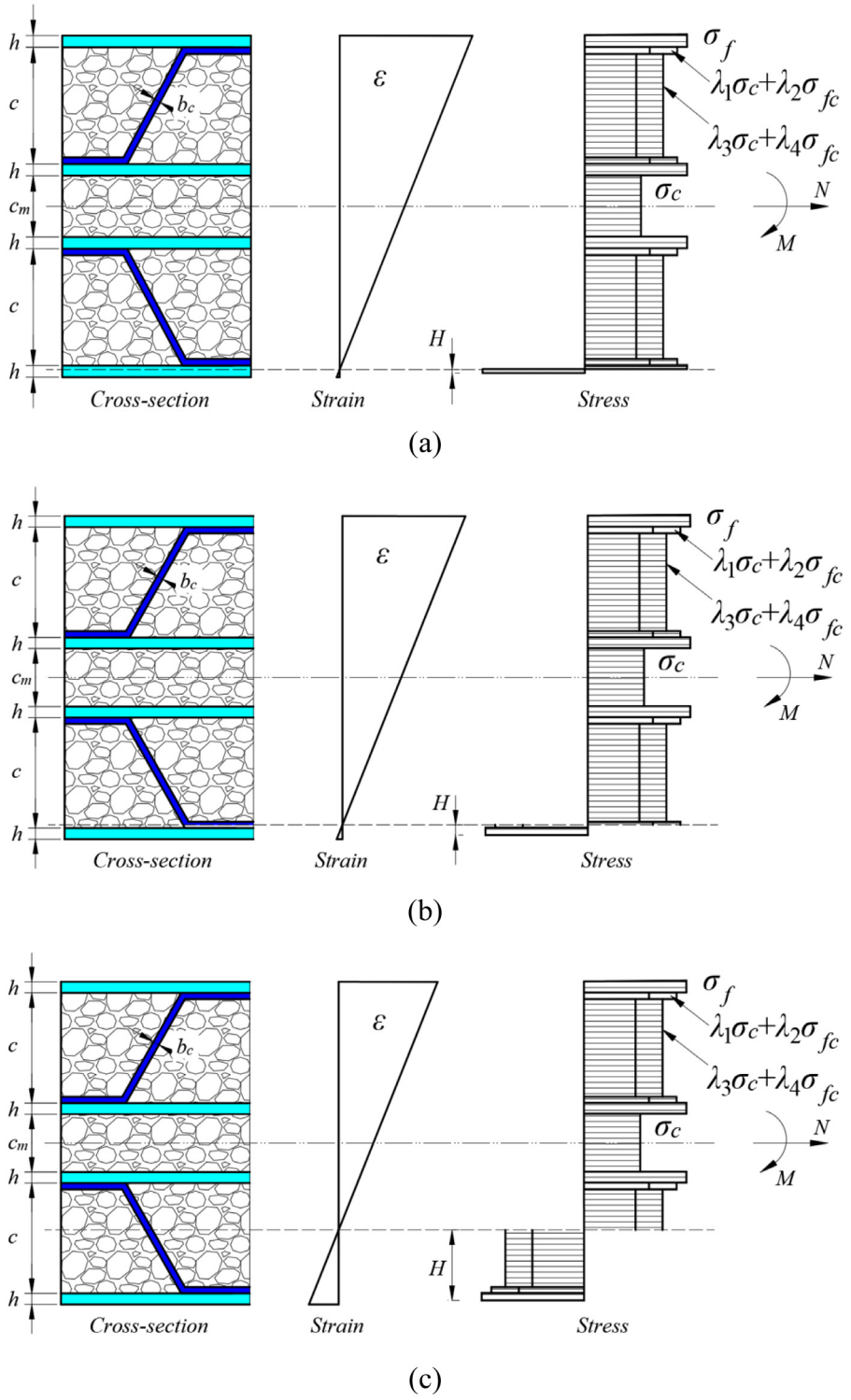

Fig. 3. Distributions of the strain and stress on cross-section for the multilayer sandwich beam with foam-filled trapezoidal corrugated and foam cores. (a) $0 \le \xi \le \frac{h}{4h+2c+c_m}$, (b) $\frac{h}{4h+2c+c_m} \le \xi \le \frac{h+b_c}{4h+2c+c_m}$, (c) $\frac{h+b_c}{4h+2c+c_m} \le \xi \le \frac{h+c-b_c}{4h+2c+c_m}$, (d) $\frac{h+c-b_c}{4h+2c+c_m} \le \xi \le \frac{h+c}{4h+2c+c_m}$, (e) $\frac{h+c}{4h+2c+c_m} \le \xi \le \frac{2h+c}{4h+2c+c_m}$, (f) $\frac{2h+c}{4h+2c+c_m} \le \xi \le \frac{1}{2}$.

multilayer sandwich beam deforms in a global manner without local denting below central punch. Thus, sandwich cross-sections retain original shape under transverse loading, and global deformation pattern for the plastic neutral axis of the multilayer sandwich beam remains straight, as shown in Fig. 5.

It is assumed that the maximum deflection of the multilayer sandwich beam under load P by the flat punch is W_0, and total extension of the left part of the multilayer sandwich beam with length $(L - a)$ is e,

$$e = e_1 + e_2 \tag{7}$$

where e_1 and e_2 are axial extensions concentrated at ends and left part for the length $(L - a)$. In Fig. 5(a), the total extension e and angular rotation can be calculated as

$$e \approx \frac{W_0^2}{2(L-a)} \tag{8}$$

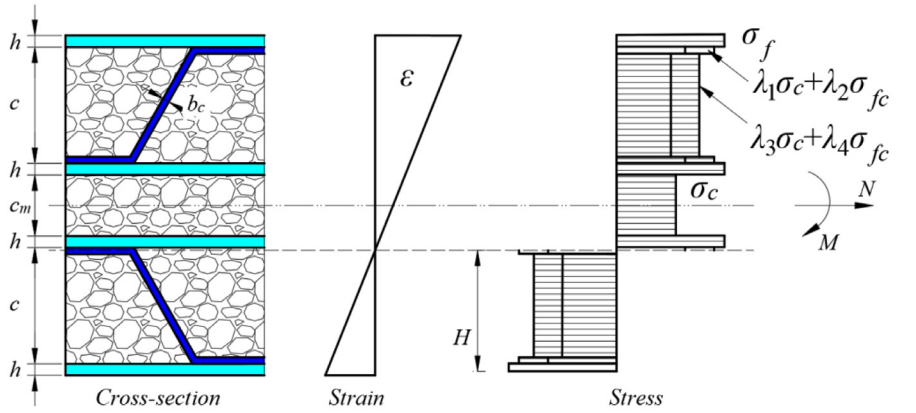

(d)

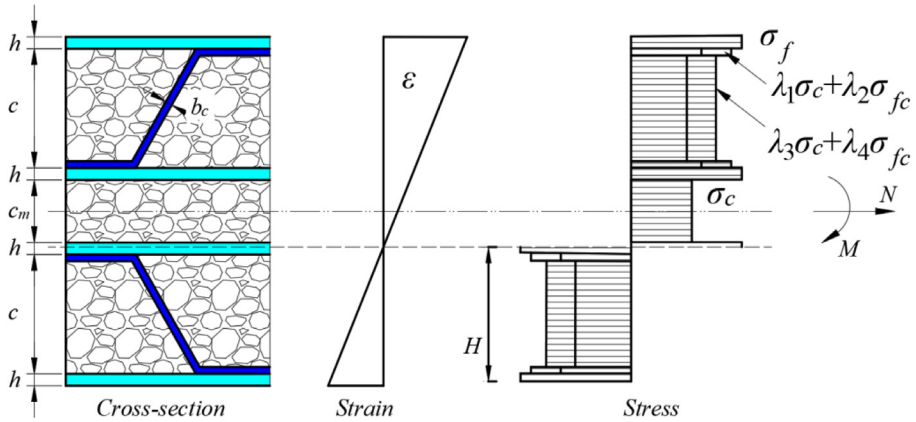

(e)

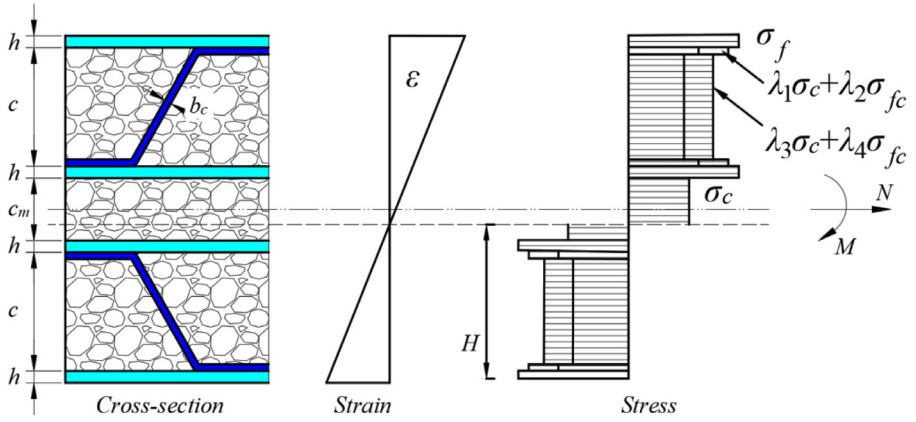

(f)

Fig. 3. (*continued*).

and

$$\psi \approx \frac{W_0}{L-a} \tag{9}$$

Based on the deformation pattern in Fig. 5(b), $M = M_m$ with M_m being the bending moment adjacent to the central punch. Thus, the moment equilibrium equation is

$$4M - P(L-a) + 2FW_0 = 0 \tag{10}$$

For the moderate deflection, $F \approx N$. When $N = 0$, $M = M_p$ and $W_0 = 0$, the global deflection of multilayer sandwich beam occur. Then, the static collapse load can be determined from Eq. (10),

$$\overline{P}_c = \frac{4M_p}{L-a} \tag{11}$$

According to the associated plastic flow rule of Eq. (5), the normality relation at ends and the points adjacent to the central punch of the

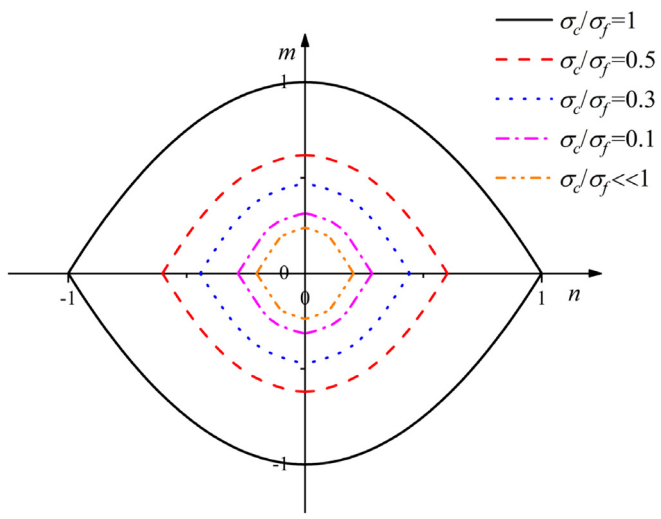

Fig. 4. The yield loci for multilayer sandwich structures with foam-filled trapezoidal corrugated and foam cores with various core strengths.

multilayer sandwich beam is

$$\frac{\dot{e}_1}{\dot{\psi}_1}=\frac{\dot{e}_2}{\dot{\psi}_2}=\begin{cases}\dfrac{(2c+c_m)A\,|n|}{2\overline{\sigma}_c}, & 0\le|n|\le\dfrac{\overline{\sigma}_c\overline{c}_m}{A}\\ \dfrac{(2c+c_m)(\overline{c}_m-\overline{\sigma}_c\overline{c}_m+A\,|n|)}{2}, & \dfrac{\overline{\sigma}_c\overline{c}_m}{A}\le|n|\le\dfrac{2\overline{h}+\overline{\sigma}_c\overline{c}_m}{A}\\ \dfrac{(2c+c_m)(C_3-2C_2+2A\,|n|)}{4\left[\overline{\sigma}_c+\overline{b}_{21}\left(\overline{\sigma}_{fc}-\overline{\sigma}_c\right)\right]}, & \dfrac{2\overline{h}+\overline{\sigma}_c\overline{c}_m}{A}\le|n|\le\dfrac{D_1}{A}\\ \dfrac{(2c+c_m)(C_6-2C_5+2A\,|n|)}{4\left[\overline{\sigma}_c+\overline{b}_c\left(\overline{\sigma}_{fc}-\overline{\sigma}_c\right)/\sin\theta\right]}, & \dfrac{D_1}{A}\le|n|\le\dfrac{D_2}{A}\\ \dfrac{(2c+c_m)(C_9-2C_8+2A\,|n|)}{4\left[\overline{\sigma}_c+\overline{b}_{21}\left(\overline{\sigma}_{fc}-\overline{\sigma}_c\right)\right]}, & \dfrac{D_2}{A}\le|n|\le\dfrac{A-2\overline{h}}{A}\\ \dfrac{(2c+c_m)(4\overline{h}+1-A+A\,|n|)}{2}, & \dfrac{A-2\overline{h}}{A}\le|n|\le1\end{cases}\tag{12}$$

From Eqs. (7), (8), (9) and (12), the relation between non-dimensional deflection W_0^* and non-dimensional axial force n of the multilayer sandwich beam is

$$W_0^*=\begin{cases}\dfrac{A\,|n|}{\overline{\sigma}_c(4\overline{h}+1)}, & 0\le|n|\le\dfrac{\overline{\sigma}_c\overline{c}_m}{A}\\ \dfrac{\overline{c}_m-\overline{\sigma}_c\overline{c}_m+A\,|n|}{4\overline{h}+1}, & \dfrac{\overline{\sigma}_c\overline{c}_m}{A}\le|n|\le\dfrac{2\overline{h}+\overline{\sigma}_c\overline{c}_m}{A}\\ \dfrac{C_3-2C_2+2A\,|n|}{C_3}, & \dfrac{2\overline{h}+\overline{\sigma}_c\overline{c}_m}{A}\le|n|\le\dfrac{D_1}{A}\\ \dfrac{C_6-2C_5+2A\,|n|}{C_6}, & \dfrac{D_1}{A}\le|n|\le\dfrac{D_2}{A}\\ \dfrac{C_9-2C_8+2A\,|n|}{C_9}, & \dfrac{D_2}{A}\le|n|\le\dfrac{A-2\overline{h}}{A}\\ \dfrac{4\overline{h}+1-A+A\,|n|}{4\overline{h}+1}, & \dfrac{A-2\overline{h}}{A}\le|n|\le1\end{cases}\tag{13}$$

where $W_0^*=W_0/(4h+2c+c_m)$. Moreover, from Eqs. (5), (10) and (13), the relation between non-dimensional load P^* and W_0^* of the multilayer sandwich beam is (Eq. (14) is given in Box I) where

$$P^*=P/P_c,$$

$$P_c=4M_p/L,$$

Table 1
The material properties of the face-sheets.

Nomenclature	Value
Yield strength σ_c	340 MPa
Elastic modulus E_f	200 GPa
Elastic Poisson's ratio ν	0.3
Linear hardening modulus E_{tf}	200 MPa

$$\overline{a}=a/L.$$

The absorbed plastic deformation energy U of the multilayer sandwich beam can be calculated as

$$U=\int_0^{W_0}P\left(W_0\right)dW_0\tag{15}$$

Define the non-dimensional plastic energy as

$$U^*=\frac{\int_0^{W_0}P\left(W_0\right)dW_0}{P_c(4h+2c+c_m)}\tag{16}$$

By substituting Eq. (15) into Eq. (16), the non-dimensional plastic energy of the multilayer sandwich beam can be obtained.

The limitations of the analytical model are listed as follows.

(1) The elasticity of the face-sheets and the metal foam and strain hardening of the face-sheets are neglected in the analytical model. The face-sheet material is assumed to be rigid-perfectly plastic material, and the metal foam is modeled as a rigid-perfectly-plastic-locking material.

(2) The face-sheets, interlayer plates, metal foam, and corrugated plates are assumed to be perfectly bonded and the fracture of the materials are not considered in the analytical model.

(3) The effect of local denting on the multilayer sandwich beams with foam-filled trapezoidal corrugated and foam cores is neglected in the analytical model.

5. Finite element analysis

Using commercial ABAQUS/Standard software, finite element (FE) simulations are conducted to investigate the large defection of fully clamped multilayer sandwich beams with foam-filled trapezoidal corrugated and foam cores under transverse loading by a flat punch at midspan. The punch is modeled as a rigid body with predefined displacement. Face-sheets, interlayer plates, metal foam, and corrugated plates are modeled by using C3D8R. A mesh sensitivity check reveal additional mesh does not change results appreciably. Symmetric boundary conditions are applied to the midspan section of the multilayer sandwich beam, and all displacements of nodes at ends of multilayer sandwich beam are zero. It is assumed that there is no friction between multilayer sandwich beam and indenter.

The width of half unit cell for the multilayer sandwich beam is b = 9 mm. The thicknesses of face-sheet is h = 1 mm, the height of foam-filled trapezoidal corrugated core is c = 4 mm, the height of the metal foam core is c_m = 4 mm, the thickness of the trapezoidal corrugated core plate is b_c = 0.5 mm. The inclination angle of the trapezoidal corrugated plate is θ = 45° and the punch width is $2a$ = 30 mm. Two half spans of multilayer sandwich beams are considered. Case A: L = 300 mm, and Case B: 450 mm.

Face-sheets, interlayer plates and corrugated plate obey J_2 flow theory of plasticity. The face-sheets, interlayer plates and corrugated plate are made of steel material with yield strength σ_f = 340 MPa, elastic modulus E_f = 200 GPa, elastic Poisson's ratio ν = 0.3, and linear hardening modulus $E_{tf}=0.001E_f$, as shown in Table 1.

Deshpande–Fleck constitutive model [42] is adopted to model crushable behavior of the metal foam in ABAQUS, which allows the shape change of yield surface due to differential hardening along the hydrostatic and deviatoric axes. The yield function of the foam core is

$$P^* = \begin{cases} \dfrac{4B + \bar{\sigma}_c(4\bar{h}+1)^2 W_0^{*2}}{4B(1-\bar{a})}, & 0 \le W_0^* \le \dfrac{\bar{c}_m}{4\bar{h}+1} \\ \dfrac{2C_1 + (4\bar{h}+1)^2 W_0^{*2} + W_0^*(4\bar{h}+1)(2\bar{c} + \bar{\sigma}_c \bar{c}_m - 1)}{2B(1-\bar{a})}, & \dfrac{\bar{c}_m}{4\bar{h}+1} \le W_0^* \le \dfrac{2\bar{h} + \bar{\sigma}_c \bar{c}_m}{4\bar{h}+1} \\ \dfrac{8C_4 + C_3(4\bar{h}+1)W_0^{*2} + (4C_2 - 2C_3)W_0^*(4\bar{h}+1)}{8B(1-\bar{a})}, & \dfrac{2\bar{h} + \bar{\sigma}_c \bar{c}_m}{4\bar{h}+1} \le W_0^* \le \dfrac{2\bar{h} + \bar{\sigma}_c \bar{c}_m + 2\bar{b}_{c1}}{4\bar{h}+1} \\ \dfrac{8C_7 + C_6(4\bar{h}+1)W_0^{*2} + (4C_5 - 2C_6)W_0^*(4\bar{h}+1)}{8B(1-\bar{a})}, & \dfrac{2\bar{h} + \bar{\sigma}_c \bar{c}_m + 2\bar{b}_{c1}}{4\bar{h}+1} \le W_0^* \le \dfrac{2\bar{h} + 1 - 2\bar{b}_{c1}}{4\bar{h}+1} \\ \dfrac{8C_{10} + C_9(4\bar{h}+1)W_0^{*2} + (4C_8 - 2C_9)W_0^*(4\bar{h}+1)}{8B(1-\bar{a})}, & \dfrac{2\bar{h} + 1 - 2\bar{b}_{c1}}{4\bar{h}+1} \le W_0^* \le \dfrac{2\bar{h}+1}{4\bar{h}+1} \\ \dfrac{(4\bar{h}+1)^2\left(1 - W_0^*\right)^2 + 2AW_0^*(4\bar{h}+1)}{4B(1-\bar{a})}, & \dfrac{2\bar{h}+1}{4\bar{h}+1} \le W_0^* \le 1 \\ \dfrac{AW_0^*(4\bar{h}+1)}{2B(1-\bar{a})}, & W_0^* \ge 1 \end{cases} \tag{14}$$

Box I.

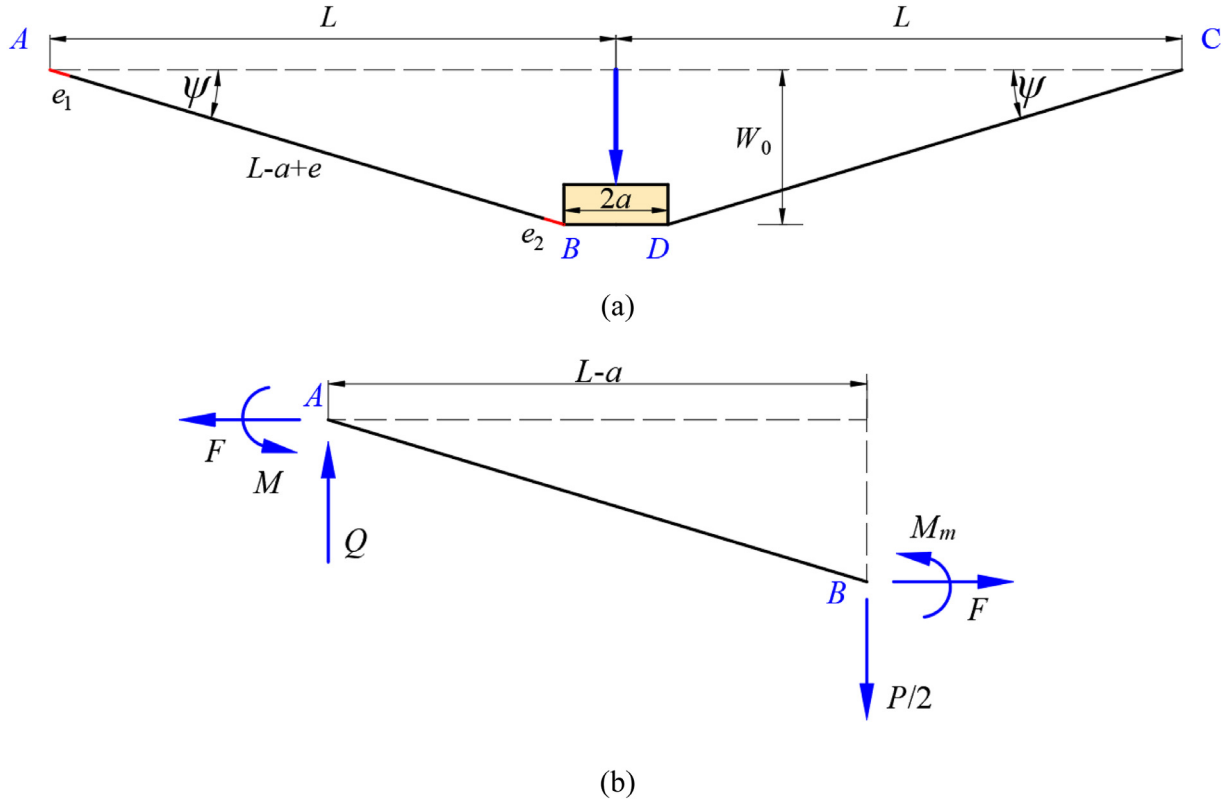

Fig. 5. Global deformation pattern of plastic neutral axis for the fully clamped multilayer sandwich beam with foam-filled trapezoidal corrugated and foam cores transversely loaded by a flat punch. (a) Deflection profile and (b) forces and moments.

$$\phi = \hat{\sigma} - \sigma_c = 0 \tag{17}$$

where

$$\hat{\sigma}^2 \equiv \frac{1}{1 + (\alpha/3)^2}\left(\sigma_e^2 + \alpha^2 \sigma_{me}^2\right) \tag{18}$$

with von Mises effective stress $\sigma_e \equiv \sqrt{3 s_{ij} s_{ij}/2}$, the deviatoric stress s_{ij}, the mean stress $\sigma_{me} \equiv \sigma_{kk}/3$ and the shape factor of yield surface α. The associated plastic flow rule is adopted and the plastic Poisson's ratio υ_p is given by

$$\upsilon_p = -\frac{\dot{\varepsilon}_{22}^p}{\dot{\varepsilon}_{11}^p} = \frac{1/2 - (\alpha/3)^2}{1 + (\alpha/3)^2} \tag{19}$$

The metal foam has yield strength $\sigma_c = 10$ MPa, elastic modulus $E_c = 2$ GPa, elastic Poisson's ratio $\upsilon_{ec} = 0.3$, plastic Poisson's ratio $\upsilon_{pc} = 0$, $\alpha = 3/\sqrt{2}$, Metal foam has a long plateau stress σ_c continuing up to densification strain $\varepsilon_D = 0.5$. It is assumed the metal foam obeys a linear hardening law with tangent modulus $E_{tc} = 20$ GPa beyond

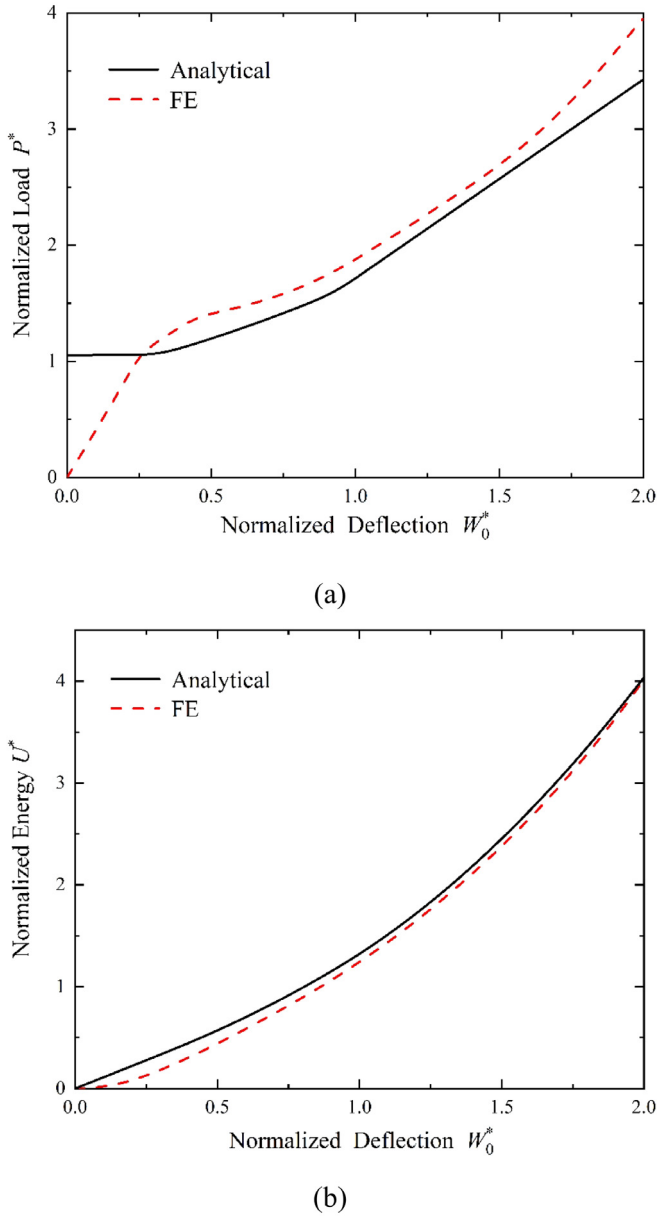

Fig. 6. Comparisons of analytical and numerical results for plastic behavior of multilayer sandwich beams with foam-filled trapezoidal corrugated and foam cores (Case A). (a) Normalized load–deflection curves, and (b) normalized energy–deflection curves.

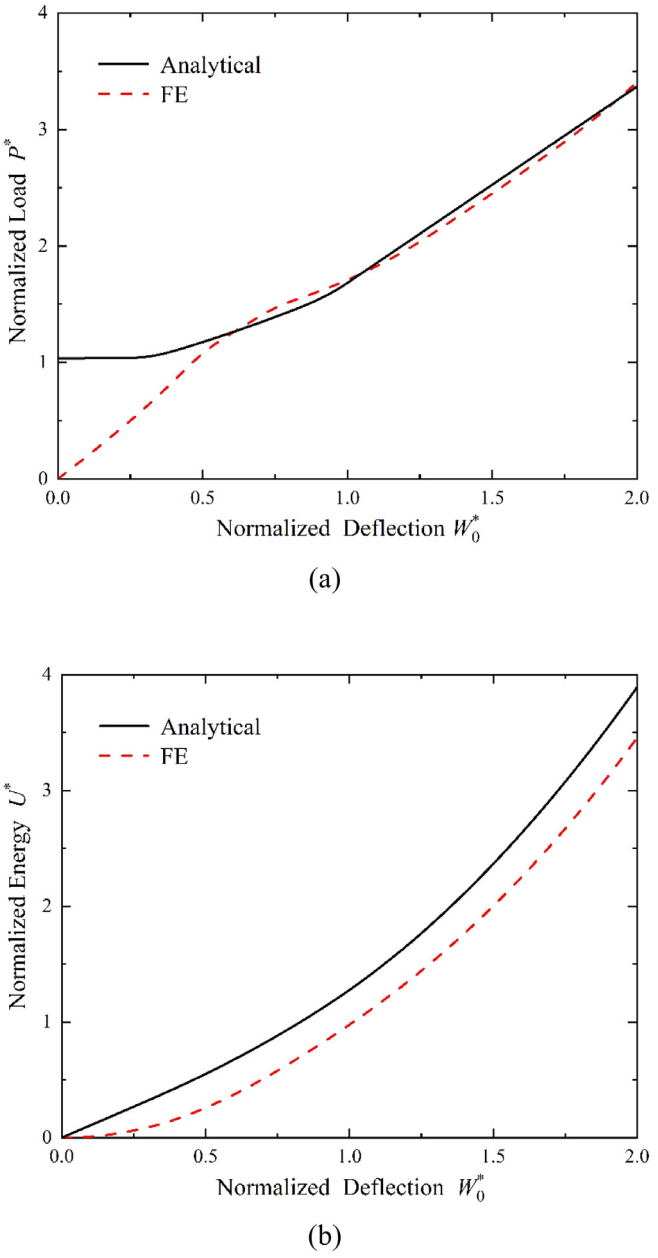

Fig. 7. Comparisons of analytical and numerical results for plastic behavior of multilayer sandwich beams with foam-filled trapezoidal corrugated and foam cores (Case B). (a) Normalized load–deflection curves, and (b) normalized energy–deflection curves.

densification. The material properties of the metal foam are listed in Table 2.

Table 2
The material properties of the metal foam.

Nomenclature	Value
Yield strength σ_f	10 MPa
Elastic modulus E_c	2 GPa
Elastic Poisson's ratio υ_{ec}	0.3
Plastic Poisson's ratio υ_{pc}	0
Linear hardening modulus E_{tc}	20 GPa
Densification strain ε_D	0.5
Shape factor of yield surface α	$3/\sqrt{2}$

6. Results and discussion

Figs. 6 and 7 show comparisons of analytical and numerical results of normalized load–deflection curves of top face-sheet and normalized energy–deflection curves of multilayer sandwich beams with foam-filled trapezoidal corrugated and foam cores under transverse loading by a flat punch. It is seen analytical results are in good agreements with numerical ones in the post yield stage. Numerical results are a little bigger than analytical ones in Fig. 6(a).

Fig. 8(a) and (b) show the Mises stress distribution of fully clamped multilayer sandwich beams with foam-filled trapezoidal corrugated and foam cores under transverse loading by a flat punch at midspan. It can be seen that the multilayer sandwich beam deforms in a global manner without obvious local denting below the indenter.

Fig. 9(a) and (b) show the effect of foam strength on load–deflection and energy–deflection curves for multilayer sandwich beams with foam-filled trapezoidal corrugated and foam cores under transverse loading by a flat punch, in which $a/L = 0.1$, $h/(2c + c_m) = 0.1$, $L/(2c + c_m) = 25$. For the given deflection, the load and the plastic energy

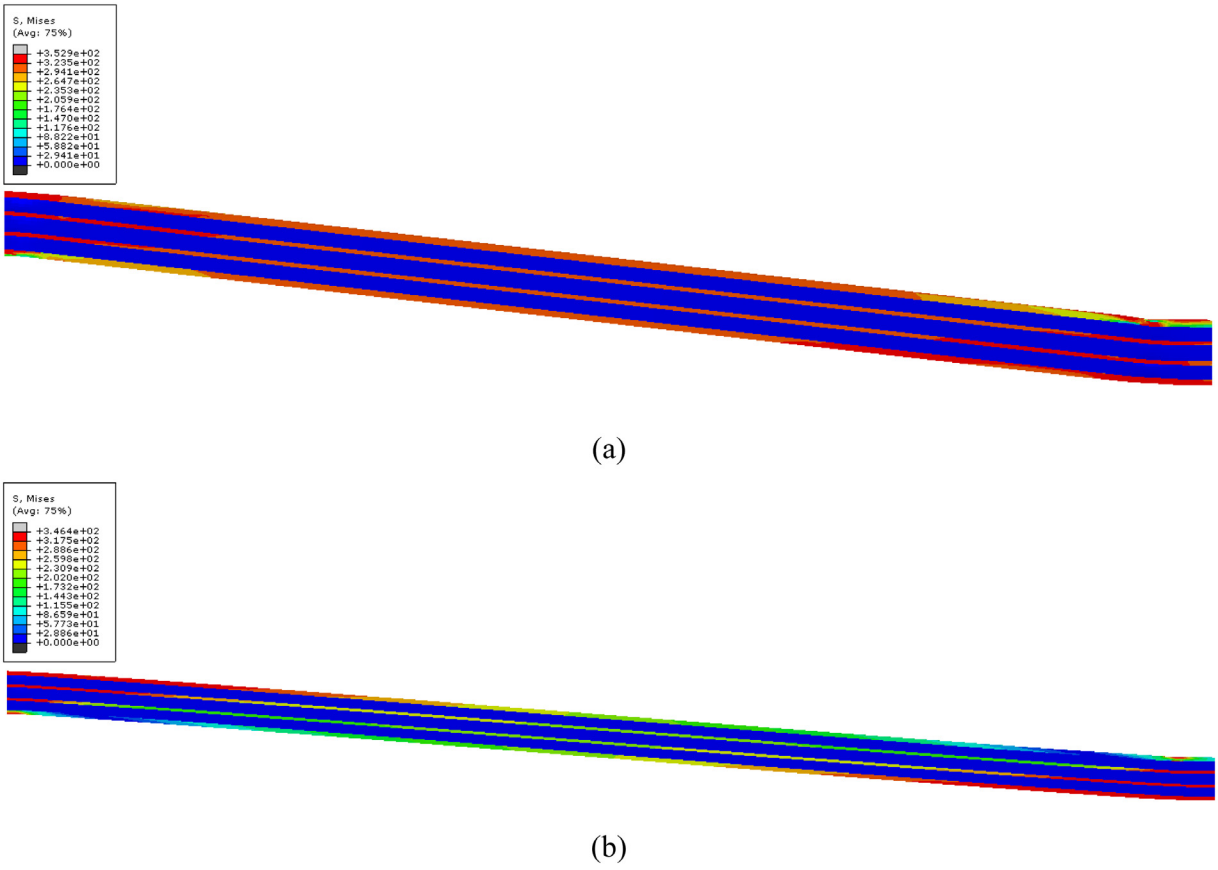

Fig. 8. The Mises stress distributions of multilayer sandwich beams with foam-filled trapezoidal corrugated and foam cores. (a) Case A, and (b) Case B.

increase with the increase of foam strength. In larger deflection, the load and plastic energy increase more significantly with the increase of foam strength. It can be seen that the foam strength has a significant influence on load-carrying capacities and energy absorption of multilayer sandwich beams with foam-filled trapezoidal corrugated and foam cores.

The effect of punch width on load–deflection and energy–deflection curves of multilayer sandwich beams with foam-filled trapezoidal corrugated and foam cores is shown in Fig. 10(a) and (b), in which $\sigma_c/\sigma_f = 0.1$, $h/(2c + c_m) = 0.1$, $L/(2c + c_m) = 25$. It is shown that for the given deflection, the load and plastic energy increase with the increase of punch width. The effect of increment of punch width on load–deflection curves are not big with the increase of the deflection in Fig. 10(a).

The effect of face-sheet thickness on load–deflection and energy–deflection curves of multilayer sandwich beams with foam-filled trapezoidal corrugated and foam cores is shown in Fig. 11(a) and (b), in which $\sigma_c/\sigma_f = 0.1$, $a/L = 0.1$, $L/(2c + c_m) = 25$. It can be seen that the face-sheet thickness has a significant influence on low-carrying capacity and energy absorption of multilayer sandwich beam, which becomes more significant in large deflection. For the given deflection, the load and plastic energy increase with the increase of face-sheet thickness.

The effect of middle foam thickness on load–deflection and energy–deflection curves of multilayer sandwich beams with foam-filled trapezoidal corrugated and foam cores is shown in Fig. 12(a) and (b), in which $\sigma_c/\sigma_f = 0.1$, $a/L = 0.1$, $h/(2c + c_m) = 0.1$. It is shown that for the given deflection, the load and plastic energy increase with the increase of middle foam thickness.

7. Conclusion

Combining the advantages of the long platform stress of metal foam, the high peak load of the corrugated sandwich structure, the multilayer sandwich beams with foam-filled trapezoidal corrugated and foam cores is designed. The plastic behavior of the fully clamped multilayer sandwich beams with foam-filled trapezoidal corrugated and foam cores under transverse loading by a flat punch is investigated analytically and numerically. The yield criterion is proposed for multilayer sandwich beams with foam-filled trapezoidal corrugated and foam cores. Based on the yield criterion, an analytical solution for large deflection of the multilayer sandwich beam with foam-filled trapezoidal corrugated and foam cores under transverse loading is obtained. The novelty of the proposed analytical model is that the contributions of the foam strength and corrugated-plate strength are considered for the proposed yield criterion of the multilayer sandwich structure with foam-filled trapezoidal corrugated and foam cores. Also, In the analytical model for the large deflection of the multilayer sandwich beam, the interaction of bending and stretching is considered. Analytical results are in good agreement with numerical ones. It is shown that the foam strength, punch size, face-sheet thickness and middle foam thickness have significant effects on the plastic behavior of multilayer sandwich beams with foam-filled trapezoidal corrugated and foam cores. The present analytical model can be used to predict the plastic behavior of multilayer sandwich beams with foam-filled trapezoidal corrugated and foam cores under transverse loading.

CRediT authorship contribution statement

Jianxun Zhang: Writing – review & editing, Writing – original draft, Visualization, Validation, Supervision, Funding acquisition, Formal analysis, Data curation, Conceptualization. **Hao Sun:** Visualization, Validation, Software, Resources, Project administration, Methodology, Investigation. **Jinlong Du:** Visualization, Validation, Software, Resources, Methodology, Investigation. **Xiaoming Liu:**

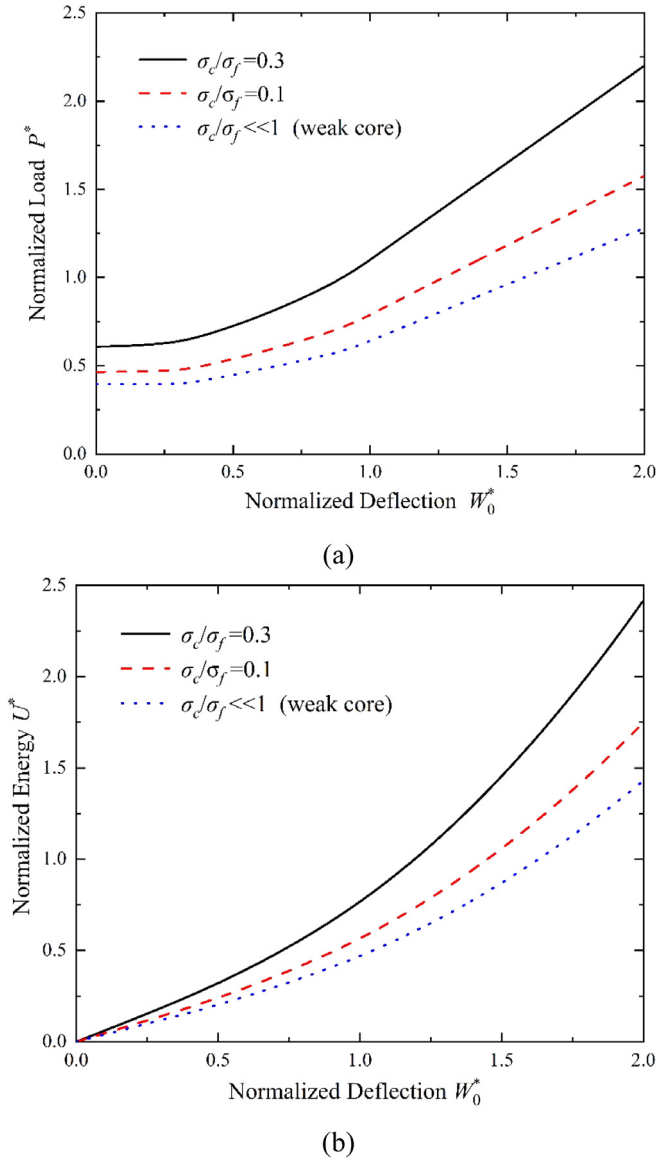

Fig. 9. Effect of foam strength on the load-carrying capacity and energy absorption of multilayer sandwich beams with foam-filled trapezoidal corrugated and foam cores. (a) Load–deflection curves and (b) energy–deflection curves.

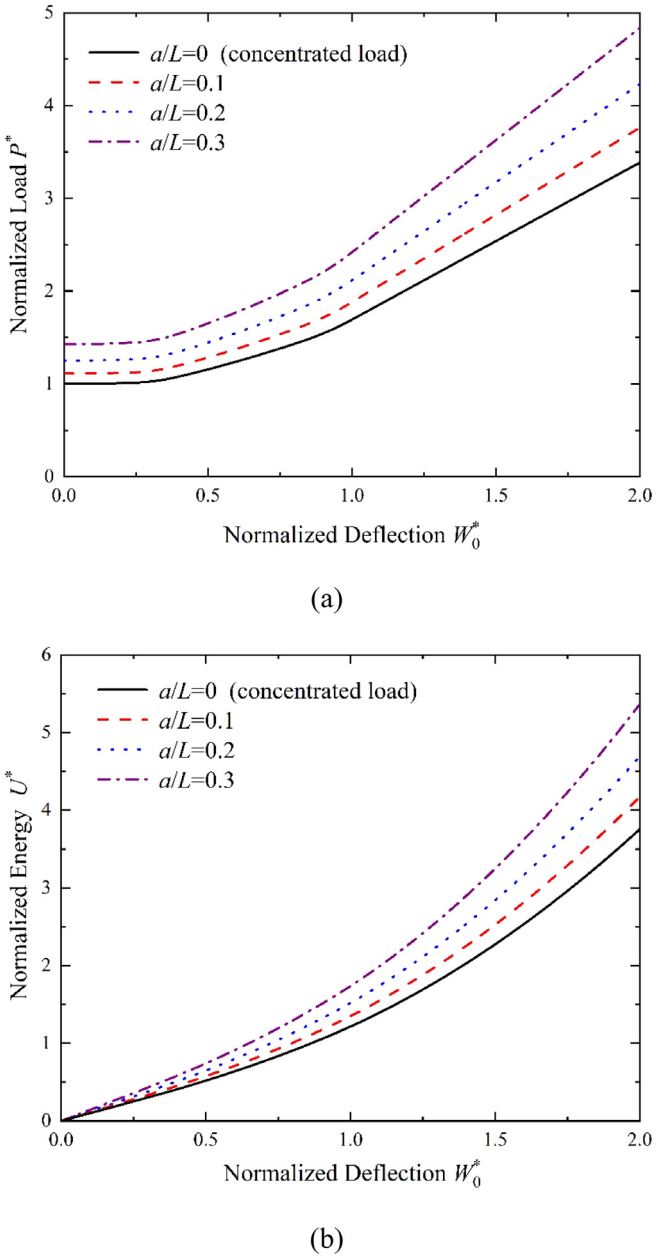

Fig. 10. Effect of punch size on the load-carrying capacity and energy absorption of multilayer sandwich beams with foam-filled trapezoidal corrugated and foam cores. (a) Load–deflection curves and (b) energy–deflection curves.

Investigation, Writing – review & editing. **Zhimin Xu:** Software. **Wei Huang:** Visualization, Validation, Software, Resources.

Declaration of competing interest

The authors declare that they have no known competing financial interests or personal relationships that could have appeared to influence the work reported in this paper.

Data availability statement

The authors attest that all data for this study are included in the paper.

Acknowledgments

The authors are grateful for their financial support through NSFC (11872291), opening fund of State Key Laboratory of Nonlinear Mechanics, China, opening project of State Key Laboratory of Structural Analysis for Industrial Equipment, China (GZ20102), the State Key Laboratory of Automotive Safety and Energy, China under Project No. KFY2202.

Appendix. The derivation of yield criterion of the multilayer sandwich cross-section with foam-filled trapezoidal corrugated and foam cores

This appendix contains the derivation of the axial force, bending moment and yield criterion of the multilayer sandwich cross-section with foam-filled trapezoidal corrugated and foam cores in detail.

In Fig. 3(b), when $\frac{h}{4h+2c+c_m} \le \xi \le \frac{h+b_c}{4h+2c+c_m}$, the axial force N and the bending moment M of the multilayer sandwich structure can be

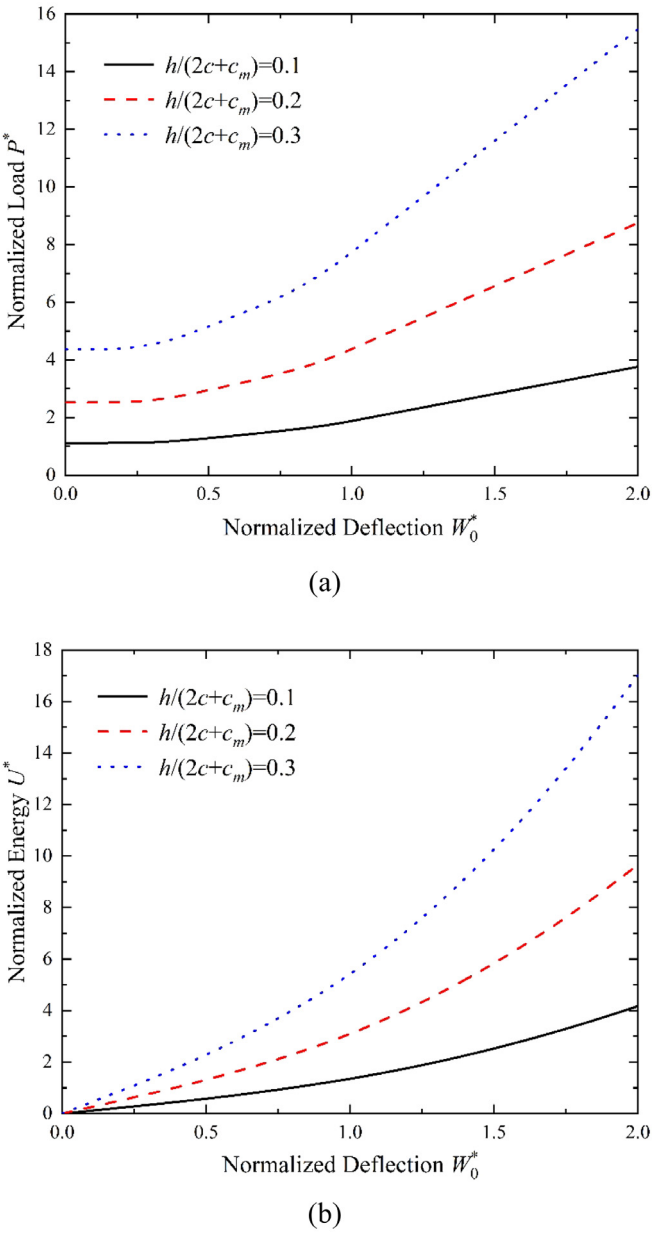

Fig. 11. Effect of face-sheet thickness on load-carrying capacity and energy absorption of multilayer sandwich beams with foam-filled trapezoidal corrugated and foam cores. (a) Load–deflection curves and (b) energy–deflection curves.

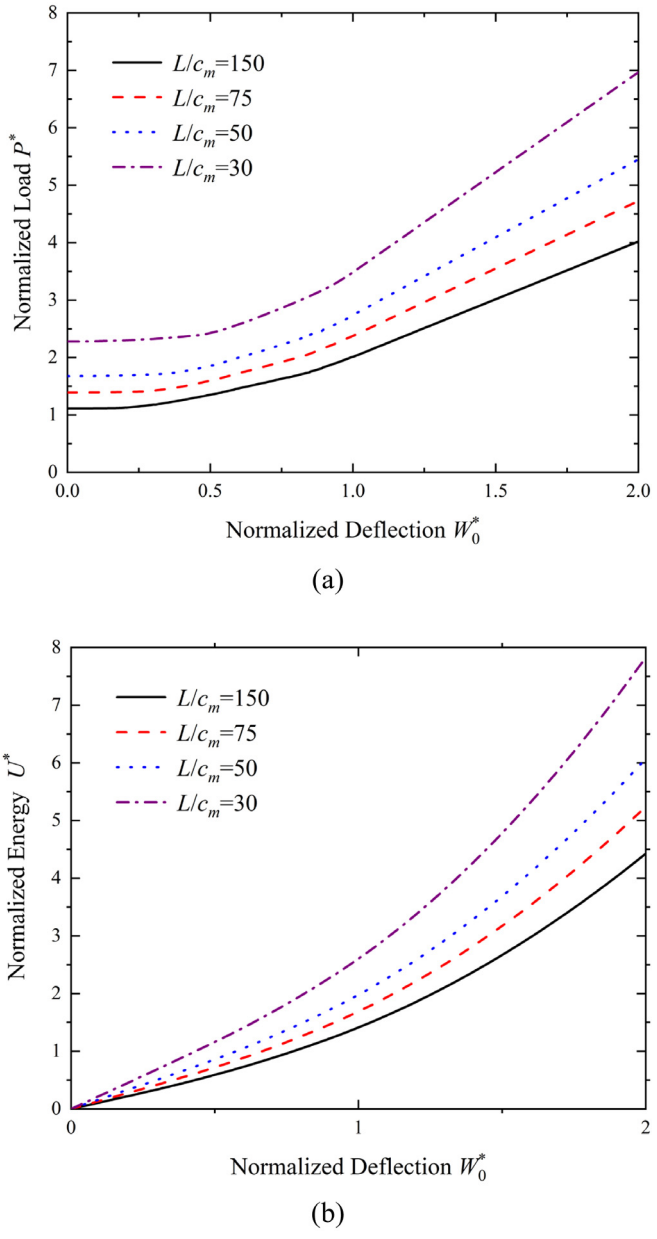

Fig. 12. Effect of middle foam thickness on load-carrying capacity and energy absorption of multilayer sandwich beams with foam-filled trapezoidal corrugated and foam cores. (a) Load–deflection curves and (b) energy–deflection curves.

expressed as

$$\begin{aligned} N &= \int_A \sigma dA = 2\sigma_f bh + 2\sigma_c b\left[c + c_m/2 + h - \xi(4h + 2c + c_m)\right] \\ &\quad +2(\sigma_{fc} - \sigma_c)\left\{b_c(b_1 + 2b_2) - b_2\left[\xi(4h + 2c + c_m) - h\right]\right\} \end{aligned} \tag{A.1}$$

and

$$\begin{aligned} M &= \int_A \sigma z dA = \sigma_f bh\left(3h + 2c + c_m\right) \\ &\quad +\frac{1}{4}\left[\sigma_c b + \left(\sigma_{fc} - \sigma_c\right) b_2\right] \\ &\quad \times\left[\left(2h + 2c + c_m\right)^2 - (1 - 2\xi)^2\left(4h + 2c + c_m\right)^2\right], \end{aligned} \tag{A.2}$$

respectively.

In Fig. 3(c), when $\frac{h+b_c}{4h+2c+c_m} \le \xi \le \frac{h+c-b_c}{4h+2c+c_m}$, the axial force N and the bending moment M of the multilayer sandwich structure can be expressed as

$$\begin{aligned} N &= \int_A \sigma dA = 2\sigma_f bh + 2\sigma_c b\left[c + c_m/2 + h - \xi\left(4h + 2c + c_m\right)\right] \\ &\quad +2(\sigma_{fc} - \sigma_c)b_c\left[b_1 + b_2 - \frac{\xi(4h + 2c + c_m) - h - b_c}{\sin\theta}\right] \end{aligned} \tag{A.3}$$

and

$$\begin{aligned} M &= \int_A \sigma z dA = \sigma_f bh\left(3h + 2c + c_m\right) \\ &\quad +\frac{1}{4}\sigma_c b\left[\left(2h + 2c + c_m\right)^2 - (1 - 2\xi)^2\left(4h + 2c + c_m\right)^2\right] \\ &\quad +\left(\sigma_{fc} - \sigma_c\right) b_c\left[\xi\left(4h + 2c + c_m\right) - h - b_c\right] \\ &\quad \times\left[(1 - \xi)\left(4h + 2c + c_m\right) - h - b_c\right] / \sin\theta \\ &\quad +\left(\sigma_{fc} - \sigma_c\right) b_c b_2\left(2h + 2c + c_m - b_c\right), \end{aligned} \tag{A.4}$$

respectively.

In Fig. 3(d), when $\frac{h_c+c-b_c}{4h+2c+c_m} \le \xi \le \frac{h+c}{4h+2c+c_m}$, the axial force N and the bending moment M of the multilayer sandwich structure can be expressed as

$$\begin{aligned} N &= \int_A \sigma dA = 2\sigma_f bh + 2\sigma_c b\left[c + c_m/2 + h - \xi(4h+2c+c_m)\right] \\ &\quad +2\left(\sigma_{fc}-\sigma_c\right) b_2\left[h + c - \xi\left(4h+2c+c_m\right)\right] \end{aligned} \tag{A.5}$$

and

$$\begin{aligned} M &= \int_A \sigma z dA = \sigma_f bh\left(3h+2c+c_m\right) \\ &\quad +\frac{1}{4}\sigma_c b\left[\left(2h+2c+c_m\right)^2 - (1-2\xi)^2\left(4h+2c+c_m\right)^2\right] \\ &\quad +\left(\sigma_{fc}-\sigma_c\right)\left[b_c b_2\left(2h+2c+c_m-b_c\right) + b_c b_1\left(2h+c+c_m\right)\right] \\ &\quad +\frac{1}{4}\left(\sigma_{fc}-\sigma_c\right) b_2\left[\left(2h+2b_c+c_m\right)^2 - (1-2\xi)^2\left(4h+2c+c_m\right)^2\right], \end{aligned} \tag{A.6}$$

respectively.

In Fig. 3(e), when $\frac{h+c}{4h+2c+c_m} \le \xi \le \frac{2h+c}{4h+2c+c_m}$, the axial force N and the bending moment M of the multilayer sandwich structure can be expressed as

$$N = \int_A \sigma dA = 2\sigma_f b\left[2h + c - \xi\left(4h+2c+c_m\right)\right] + \sigma_c b c_m \tag{A.7}$$

and

$$\begin{aligned} M &= \int_A \sigma z dA \\ &= \sigma_f b\left\{h\left(3h+2c+c_m\right) + \frac{1}{4}\left[\left(2h+c_m\right)^2 - (1-2\xi)^2\left(4h+2c+c_m\right)^2\right]\right\} \\ &\quad +\left[\sigma_c bc + \left(\sigma_{fc}-\sigma_c\right) b_c\left(b_1+2b_2\right)\right]\left(2h+c+c_m\right), \end{aligned} \tag{A.8}$$

respectively.

In Fig. 3(f), when $\frac{2h+c}{4h+2c+c_m} \le \xi \le \frac{1}{2}$, the axial force N and the bending moment M of the multilayer sandwich structure can be expressed as

$$N = \int_A \sigma dA = \sigma_c b\left(4h+2c+c_m\right)(1-2\xi) \tag{A.9}$$

and

$$\begin{aligned} M &= \int_A \sigma z dA = \sigma_f bh\left(4h+2c+2c_m\right) \\ &\quad +\frac{1}{4}\sigma_c b\left[c_m^2 - (1-2\xi)^2\left(4h+2c+c_m\right)^2\right] \\ &\quad +\left[\sigma_c bc + \left(\sigma_{fc}-\sigma_c\right) b_c\left(b_1+2b_2\right)\right]\left(2h+c+c_m\right), \end{aligned} \tag{A.10}$$

respectively.

Combination of Eqs. (1) to (4) and (A.1) to (A.10) leads to

$$n = \begin{cases} 1 - \dfrac{2\xi(1+4\overline{h})}{A}, & 0 \le \xi \le \dfrac{h}{4h+2c+c_m} \\ \dfrac{C_8 - \xi C_9}{A}, & \dfrac{h}{4h+2c+c_m} \le \xi \le \dfrac{h+b_c}{4h+2c+c_m} \\ \dfrac{C_5 - \xi C_6}{A}, & \dfrac{h+b_c}{4h+2c+c_m} \le \xi \le \dfrac{h+c-b_c}{4h+2c+c_m} \\ \dfrac{C_2 - \xi C_3}{A}, & \dfrac{h_c+c-b_c}{4h+2c+c_m} \le \xi \le \dfrac{h+c}{4h+2c+c_m} \\ \dfrac{4\overline{h} + 2\overline{c} + \overline{\sigma}_c\overline{c}_m - 2\xi\left(4\overline{h}+1\right)}{A}, & \dfrac{h+c}{4h+2c+c_m} \le \xi \le \dfrac{2h+c}{4h+2c+c_m} \\ \dfrac{\overline{\sigma}_c\left(4\overline{h}+1\right)(1-2\xi)}{A}, & \dfrac{2h+c}{4h+2c+c_m} \le \xi \le \dfrac{1}{2} \end{cases} \tag{A.11}$$

and

$$m = \begin{cases} \dfrac{\left(4\overline{h}+1\right)\left(\xi-\xi^2\right)}{B} & 0 \le \xi \le \dfrac{h}{4h+2c+c_m} \\ \dfrac{8C_{10} - C_9\left(4\overline{h}+1\right)(1-2\xi)^2}{8B} & \dfrac{h}{4h+2c+c_m} \le \xi \le \dfrac{h+b_c}{4h+2c+c_m} \\ \dfrac{8C_7 - C_6\left(4\overline{h}+1\right)(1-2\xi)^2}{8B}, & \dfrac{h+b_c}{4h+2c+c_m} \le \xi \le \dfrac{h+c-b_c}{4h+2c+c_m} \\ \dfrac{8C_4 - C_3\left(4\overline{h}+1\right)(1-2\xi)^2}{8B}, & \dfrac{h_c+c-b_c}{4h+2c+c_m} \le \xi \le \dfrac{h+c}{4h+2c+c_m} \\ \dfrac{4C_1 - \left(4\overline{h}+1\right)^2(1-2\xi)^2}{4B}, & \dfrac{h+c}{4h+2c+c_m} \le \xi \le \dfrac{2h+c}{4h+2c+c_m} \\ 1 - \dfrac{\overline{\sigma}_c\left(4\overline{h}+1\right)^2(1-2\xi)^2}{4B}, & \dfrac{2h+c}{4h+2c+c_m} \le \xi \le \dfrac{1}{2} \end{cases} \tag{A.12}$$

where

$n = N/N_P$,
$m = M/M_P$,
$\overline{\sigma}_{fc} = \sigma_{fc}/\sigma_f$,
$\overline{\sigma}_c = \sigma_c/\sigma_f$,
$\overline{h} = h/\left(2c+c_m\right)$,
$\overline{c} = c/\left(2c+c_m\right)$,
$\overline{c}_m = c_m/\left(2c+c_m\right)$,
$\overline{b}_c = b_c/b$,
$\overline{b}_{c1} = b_c/\left(2c+c_m\right)$,
$\overline{b}_1 = b_1/\left(2c+c_m\right)$,
$\overline{b}_2 = b_2/\left(2c+c_m\right)$,
$\overline{b}_{11} = b_1/b$,
$\overline{b}_{21} = b_2/b$.

References

[1] J. Zhang, Q. Qin, W. Ai, Z. Wang, T.J. Wang, Indentation of metal foam core sandwich beams: Experimental and theoretical investigations, Exp. Mech. 56 (2016) 771–784.
[2] Z. Shi, Y.F. Zhong, Q.S. Yi, X. Peng, High efficiency analysis model for composite honeycomb sandwich plate by using variational asymptotic method, Thin Wall. Struct. 163 (2021) 107709.
[3] J.S. Yang, J. Xiong, L. Ma, L.N. Feng, S.Y. Wang, L.Z. Wu, Modal response of all-composite corrugated sandwich cylindrical shells, Compos. Sci. Technol. 115 (2015) 9–20.
[4] J.X. Zhang, Q.H. Qin, T.J. Wang, Compressive strengths and dynamic response of corrugated metal sandwich plates with unfilled and foam-filled sinusoidal plate cores, Acta Mech. 224 (2013) 759–775.
[5] G.Y. Sun, X.T. Huo, D.D. Chen, Q. Li, Experimental and numerical study on honeycomb sandwich panels under bending and in-panel compression, Mater. Des. 133 (2017) 154–168.
[6] L. Jing, K. Liu, X.Y. Su, X. Guo, Experimental and numerical study of square sandwich panels with layered-gradient foam cores to air-blast loading, Thin Wall. Struct. 161 (2021) 107445.
[7] L.J. Feng, G.T. Wei, G.C. Yu, L.Z. Wu, Underwater blast behaviors of enhanced lattice truss sandwich panels, Int. J. Mech. Sci. 150 (2019) 238–246.
[8] J.X. Zhang, Q.H. Qin, C.P. Xiang, T.J. Wang, Plastic analysis of multilayer sandwich beams with metal foam cores, Acta Mech. 227 (2016) 2477–2491.
[9] H.X. Wu, X.C. Zhang, Y. Liu, In-plane crushing behavior of density graded cross-circular honeycombs with zero Poisson's ratio, Thin Wall. Struct. 151 (2020) 106767.
[10] B.O. Baba, Curved sandwich composites with layer-wise graded cores under impact loads, Compos. Struct. 159 (2017) 1–11.
[11] M.F. Ashby, A.G. Evans, N.A. Fleck, L.J. Gibson, J.W. Hutchinson, H.N.G. Wadley, Metal Foams: A Design Guide, Butterworth Heinemann, Oxford, 2000.

[12] M.R.M. Rejab, W.J. Cantwell, The mechanical behaviour of corrugated-core sandwich panels, Composites B 47 (2013) 267–277.
[13] D.M. Wang, Cushioning properties of multi-layer corrugated sandwich structures, J. Sandwich Struct. Mater. 11 (2009) 57–66.
[14] L.J. Gibson, M.F. Ashby, Cellular Solids: Structure and Properties, Pergamon Press, Oxford, 1997.
[15] V.L. Tagarielli, N.A. Fleck, V.S. Deshpande, Collapse of clamped and simply supported composite sandwich beams in three-point bending, Composites B 35 (2004) 523–534.
[16] J.L. Yu, E.H. Wang, J.R. Li, Z.J. Zheng, Static and low-velocity impact behavior of sandwich beams with closed-cell aluminum-foam core in three-point bending, Int. J. Impact Eng. 35 (2008) 885–894.
[17] V. Crupi, G. Epasto, E. Guglielmino, Collapse modes in aluminium honeycomb sandwich panels under bending and impact loading, Int. J. Impact Eng. 43 (2012) 6–15.
[18] L. Jing, Z.H. Wang, L.M. Zhao, Failure and deformation modes of sandwich beams under quasi-static loading, Appl. Mech. Mater. 29–32 (2010) 84–88.
[19] G.Q. Zhang, B. Wang, L. Ma, J. Xiong, L.Z. Wu, Response of sandwich structures with pyramidal truss cores under the compression and impact loading, Compos. Struct. 100 (2013) 451–463.
[20] B.H. Jiang, Z.B. Li, F.Y. Lu, Failure mechanism of sandwich beams subjected to three-point bending, Compos. Struct. 133 (2015) 739–745.
[21] A.A. Nia, M.Z. Sadeghi, The effects of foam filling on compressive response of hexagonal cell aluminum honeycombs under axial loading-experimental study, Mater. Des. 31 (2010) 1216–1230.
[22] M.Z. Mahmoudabadi, M. Sadighi, A study on the static and dynamic loading of the foam filled metal hexagonal honeycomb - theoretical and experimental, Mater. Sci. Eng. A 530 (2011) 333–343.
[23] V.N. Burlayenko, T. Sadowski, Effective elastic properties of foam-filled honeycomb cores of sandwich panels, Compos. Struct. 92 (2010) 2890–2900.
[24] G.Q. Zhang, B. Wang, L. Ma, L.Z. Wu, S.D. Pan, J.S. Yang, Energy absorption and low velocity impact response of polyurethane foam filled pyramidal lattice core sandwich panels, Compos. Struct. 108 (2014) 304–310.
[25] J.X. Zhang, Q.H. Qin, T.J. Wang, Compressive strengths and dynamic response of corrugated metal sandwich plates with unfilled and foam-filled sinusoidal plate cores, Acta Mech. 224 (2013) 759–775.
[26] Q.H. Qin, W. Zhang, S.Y. Liu, J.F. Li, J.X. Zhang, L.H. Poh, On dynamic response of corrugated sandwich beams with metal foam-filled folded plate core subjected to low-velocity impact, Compos. A 114 (2018) 107–116.
[27] Y.C. Fu, P. Sadeghian, Flexural and shear characteristics of bio-based sandwich beams made of hollow and foam-filled paper honeycomb cores and flax fiber composite skins, Thin Wall. Struct. 153 (2020) 106834.
[28] J.B. Sha, T.H. Yip, In situ surface displacement analysis on sandwich and multilayer beams composed of aluminum foam core and metallic face sheets under bending loading, Mater. Sci. Eng. A 386 (2004) 91–103.
[29] N.A. Apetre, B.V. Sankar, D.R. Ambur, Low-velocity impact response of sandwich beams with functionally graded core, Int. J. Solids Struct. 43 (2006) 2479–2496.
[30] J. Xiong, A. Vaziri, L. Ma, J. Papadopoulos, L. Wu, Compression and impact testing of two-layer composite pyramidal-core sandwich panels, Compos. Struct. 94 (2012) 793–801.
[31] C. Kilicaslan, M. Guden, I.K. Odaci, A. Tasdemirci, Experimental and numerical studies on the quasi-static and dynamic crushing responses of multi-layer trapezoidal aluminum corrugated sandwiches, Thin Wall. Struct. 78 (2014) 70–78.
[32] S.J. Hou, C.F. Shu, S.Y. Zhao, T.Y. Liu, X. Han, Q. Li, Experimental and numerical studies on multi-layered corrugated sandwich panels under crushing loading, Compos. Struct. 126 (2015) 371–385.
[33] B.T. Cao, B. Hou, Y.L. Li, H. Zhao, An experimental study on the impact behavior of multilayer sandwich with corrugated cores, Int. J. Solids Struct. 109 (2017) 33–45.
[34] J.X. Zhang, Y. Ye, Q.H. Qin, Large deflections of multilayer sandwich beams with metal foam cores under transverse loading, Acta Mech. 229 (2018) 2585–3599.
[35] P. Zhou, Y. Liu, X.Y. Liang, Analytical solutions for large deflections of functionally graded beams based on layer-graded beam model, Int. J. Appl. Mech. 10 (2018) 1850098.
[36] W. Ferdous, A. Manalo, T. Aravinthan, A. Fam, Flexural and shear behaviour of layered sandwich beams, Constr. Build. Mater. 173 (2018) 429–442.
[37] Z.J. Li, W.S. Chen, H. Hao, Dynamic crushing and energy absorption of foam filled multi-layer folded structures: Experimental and numerical study, Int. J. Impact Eng. 133 (2019) 103341.
[38] C.F. Shu, S.J. Hou, Y.X. Zhang, Y.T. Luo, Crashworthiness analysis and optimization of different configurations multi-layered corrugated sandwich panels under crush loading, J. Sandwich Struct. Mater. 23 (2021) 2901–2922.
[39] X.F. Zhou, L. Jing, Deflection analysis of clamped square sandwich panels with layered-gradient foam cores under blast loading, Thin Wall. Struct. 157 (2020) 107141.
[40] L. MacDonnell, P. Sadeghian, Experimental and analytical behaviour of sandwich composites with glass fiber-reinforced polymer facings and layered fiber mat cores, J. Compos. Mater. 54 (2020) 4875–4887.
[41] J.B. Martin, Plasticity: Fundamentals and General Results, The MIT Press, 1975.
[42] V.S. Deshpande, V.S. Fleck, Isotropic constitutive models for metallic foams, J. Mech. Physics Solids. 48 (2000) 1253–1283.